

Copyright ©2008 IEEE.

Reprinted from:

# Capacity of Ad Hoc Networks with Line Topology Based on UWB and WLAN Technologies

Samer Bali

Institute of Comm. Technology  
Leibniz University of Hanover.  
bali@ikt.uni-hannover.de

Jan Steuer

DOK Systems Company of Comm.  
Technology Ltd.  
jan.steuer@doksysteme.de

Klaus Jobmann

Institute of Comm. Technology  
Leibniz University of Hanover.  
jo@ikt.uni-hannover.de

**Submitted on 05.04.2008 to Wireless Telecommunications Symposium 2008.**

This material is posted here with permission of the IEEE. Internal or personal use of this material is permitted. However, permission to reprint/republish this material for advertising or promotional purposes or for creating new collective works for resale or redistribution must be obtained from the IEEE by writing to [pubs-permissions@ieee.org](mailto:pubs-permissions@ieee.org).

**By choosing to view this document, you agree to all provisions of the copyright laws protecting it.**

# Capacity of Ad Hoc Networks with Line Topology Based on UWB and WLAN Technologies

Samer Bali

Institute of Comm. Technology  
Leibniz University of Hanover.  
bali@ikt.uni-hannover.de

Jan Steuer

DOK Systems Company of Comm.  
Technology Ltd.  
jan.steuer@doksysteme.de

Klaus Jobmann

Institute of Comm. Technology  
Leibniz University of Hanover.  
jo@ikt.uni-hannover.de

**Abstract** - In this paper a systematic model is used to find a closed-form formula for the channel capacity of ad hoc networks with line topology based on Ultra-Wideband (UWB) and Wireless Local Area Network (WLAN) technologies. As a result, it has been found that the interference level in this network topology is upper bounded and a formula to compute this limit is provided. Based on our computations, it is shown that UWB ad hoc networks have much larger channel capacity than WLAN ad hoc networks. With UWB technology the maximum throughput per node is limited by the transmission bit rate while it is limited by the low channel capacity when WLAN technology is used. As a minor advantage of our findings, a clue about routing algorithm optimization is also given.

## I. INTRODUCTION

In ad hoc networks, communication between nodes is established via wireless links. Nodes can use this link according to a certain medium access scheme. All nodes of ad hoc networks operate as routers to forward packets for other nodes. Thus a multi-hop communications network is formed. In addition, as nodes can move freely, topological changes are very often. Channel capacity is an important parameter in the evaluation and design of ad hoc networks. Analytical computation of channel capacity of ad hoc networks is a very difficult task since it depends on many factors such as channel model, network topology, medium access, routing mechanism and traffic pattern. So, some assumptions should be made to simplify mathematical derivation. Good assumptions may lead to results that can be generalized.

This paper focuses on channel capacity computation of ad hoc networks with line topology since it can be used in vital industrial indoor applications, e.g., a production line in a factory. A viable production line network scenario is described in [1]. Ultra-Wideband (UWB) is a new transmission technique that is supposed to replace Wireless Local Area Network (WLAN) transmission techniques in multi-hop ad hoc networks in short range scenarios. Hence, a comparison of channel capacity of ad hoc networks based on these two technologies is also presented. The rest of the paper is organized as follows. Section II presents some related works. Section III describes our model approach. In section IV the mathematical derivation of channel capacity is presented and comparisons are performed. Model verification is presented in section V. Restrictions of our model are discussed in section

VI. Finally, we summarize and conclude our work in section VII.

## II. RELATED WORK

In the last few years there has been a great interest in computing the channel capacity of ad hoc networks using analytical calculations. For example, in [2] the authors found asymptotic values for the throughput capacity per node in ad hoc networks in which the nodes are uniformly distributed on a unit disk. With similar network topology, the authors of [3] found also asymptotic values for the throughput capacity per node but they considered a different communication model in which each node has a limited transmission power and uses a huge bandwidth such as in UWB communications. In [4] the authors propose a new model to find a closed-form formula for interference level and channel capacity in ad hoc networks with honey-grid configuration based on WLAN technology. In contrast to [2] and [3], a closed-form formula for channel capacity of ad hoc networks with line topology is found in this paper using a systematic model based on the model proposed in [4]. With this model, the effects of spreading-spectrum techniques and medium access schemes on channel capacity can be easily determined.

## III. MODEL DESCRIPTION

### A. Radio Propagation Assumptions

For simplicity of mathematical derivations, we will use the pathloss power law model for radio propagation [5]. In this model, the average power in Watts of a signal at a certain distance  $d$  from the transmitter is given by:

$$P(d) = c(d)^{-\beta} \quad (1)$$

where  $\beta$  is the pathloss exponent and  $c$  is a constant that determines the average power level of transmission. The transmission range of a node denoted by  $R$  determines the coverage area of that node. With the power law model, the coverage area of a node is limited by a circle with radius  $R$ . A node has a direct link with all other nodes that are positioned within its coverage area.

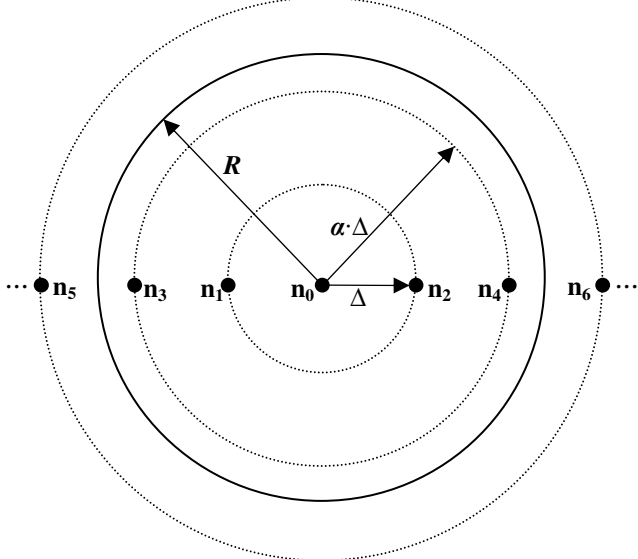


Fig. 1: Line Topology Configuration.

### B. Topology Assumptions

We will assume that nodes are uniformly distributed along a line topology. Fig. 1 shows our line topology in which each node has 2 adjacent nodes at the same distance  $\Delta$  with opposite directions. From the view point of node  $n_0$  in the center of line topology, other nodes are placed on the diameter endpoints of co-centered rings, represented by dotted circles, along the same line. The  $j^{\text{th}}$  ring has a radius of  $j \cdot \Delta$  and contains 2 nodes. The size of the network can be expressed in terms of the total number of nodes  $N$ , or by  $K$  rings around node  $n_0$ .  $N$  and  $K$  are related to each other by:

$$N = 1 + 2K \quad (2)$$

$$K = \frac{N - 1}{2}; \quad N \text{ is odd} \quad (3)$$

For example,  $N$  is 7 and  $K$  is 3 in Fig. 1. The coverage area of node  $n_0$  is represented by a solid circle of radius  $R$  and includes 2 rings as shown in Fig. 1. The coverage area could be larger and includes more rings. However, the radius  $R$  cannot be less than  $\Delta$ , otherwise, the network would not be connected. We will assume that all other nodes have the same coverage area radius as node  $n_0$ . Let  $\alpha$  be the number of rings included in the coverage area of a node. For example,  $\alpha$  is 2 in Fig. 1. For fixed  $R$ , the density of nodes in the network can be increased by increasing the value of  $\alpha$ .

### C. Medium Access Assumptions

On the data link layer, we will assume that the network uses a Medium Access Control (MAC) with Time-Hopping (TH) such as TH Impulse-Radio UWB (TH-IR-UWB) [6]. In this multiple access scheme, all nodes are allowed to transmit simultaneously since a unique TH code is assigned to each node. Even in the lack of synchronization between nodes,

collisions are unlikely to occur since the duty cycle of UWB signal is very small. Hence, all nodes in the network can transmit simultaneously with very low interference level.

For comparison, we will consider also the basic form of the Carrier Sense Multiple Access with Collision Avoidance (CSMA/CA) used in WLAN. According to this multiple access scheme, if a node is transmitting, all other nodes inside the coverage area should not transmit simultaneously [7], i.e., a certain distance (or hop count) between simultaneous transmitting nodes should exist. Thus, the interference level from other nodes will be reduced. However, an additional restriction on channel capacity will be imposed by this MAC protocol [4] as we will see in section IV.

### D. Routing Assumptions

Each node can communicate directly with all nodes inside its coverage area. To communicate with other destinations, multi-hopping must be used. In multi-hop communications there are basically two ways to reach destinations. For example, in Fig. 1, if node  $n_0$  wishes to communicate with node  $n_6$  on the third ring seen from the center node  $n_0$ , it either can hop through node  $n_2$  on the first ring and then node  $n_4$  on the second ring; or it can skip the first ring and hop directly to node  $n_4$  on the second ring before reaching the destination node  $n_6$ . The first method conserves energy while the second method keeps the hop-count to a minimum. Our model will consider both methods by controlling the value of  $\alpha$ . The energy conservation method is considered if  $\alpha$  is 1. Otherwise, the minimum hop-count method is considered.

All rings that can be used for multi-hop routing will be called relay rings and nodes on them will be called relay nodes. Generally, if there are  $\alpha$  rings inside the coverage area of node  $n_0$  in Fig. 1, the number of relay nodes including the source node  $n_0$  is then:

$$N_r = 1 + 2 \lfloor K / \alpha \rfloor \quad (4)$$

where  $\lfloor K / \alpha \rfloor$  is the number of co-centered relay rings seen from node  $n_0$  and  $\lfloor X \rfloor$  denotes the integer part of  $X$ .

### E. Traffic Assumptions

The output traffic per node consists of new traffic that the node generates and relay traffic that the node relays for other nodes. New traffic generated per node will be called the input throughput per node denoted by  $r_{in}$ . Also, the output traffic per node will be called the output throughput per node denoted by  $r_o$ . We will assume that the new traffic is generated by all nodes independently and according to Poisson distribution. Let  $\lambda$  be the average value of new traffic measured in packet per time-slot  $t_s$  per node.  $t_s$  is actually the time duration of one data packet and it is determined by the transmission bit rate  $r$  (in bits/s) and the data packet size  $P_s$  (in bits) as following:

$$t_s = P_s / r \quad (5)$$

Hence,  $\lambda / t_s$  is the average number of packet transmissions per second. The probability of  $k$  packet transmissions during  $t$  time interval is then:

$$Pr_k(t, \lambda) = \frac{(t \cdot \lambda / t_s)^k}{k!} \exp(-t \cdot \lambda / t_s) \quad (6)$$

Let  $E[\mathbf{h}]$  be the expected hop-count of the network. A closed-form formula of  $E[\mathbf{h}]$  will be derived in the following subsection. For any source-destination pair in the network, there is an average of  $E[\mathbf{h}]-1$  relay nodes between them. Hence, the expected amount of relay traffic at any node is  $\lambda(E[\mathbf{h}]-1)$ . As a result, the average value of the output traffic per node  $\lambda_{tot}$  is:

$$\begin{aligned} \lambda_{tot} &= \lambda + \lambda(E[\mathbf{h}]-1) \\ &= \lambda \cdot E[\mathbf{h}] \end{aligned} \quad (7)$$

Hence, the probability of packet transmission per node  $p_{tr}$  can be calculated using equation (6) as following:

$$\begin{aligned} p_{tr} &= 1 - Pr_0(t_s, \lambda_{tot}) \\ &= 1 - \exp(-\lambda \cdot E[\mathbf{h}]) \end{aligned} \quad (8)$$

Finally,  $r_{in}$  and  $r_o$  can be related to each other as following:

$$\begin{aligned} r_{in} &= P_s \cdot \lambda / t_s \\ &= \lambda \cdot r \end{aligned} \quad (9)$$

$$\begin{aligned} r_o &= P_s \cdot \lambda_{tot} / t_s \\ &= \lambda \cdot E[\mathbf{h}] \cdot r \\ &= E[\mathbf{h}] \cdot r_{in} \end{aligned} \quad (10)$$

From equation (10), we can find the maximum allowed input throughput per node  $r_{in,max}$  as following:

$$r_{in,max} = \frac{r_{o,max}}{E[\mathbf{h}]} \quad (11)$$

where  $r_{o,max}$  is the maximum output throughput per node and it is determined by the channel capacity.

#### F. Expected Hop-Count

To find  $E[\mathbf{h}]$  as a function of number of nodes, the exact hop-count distribution  $\mathbf{h}$  of the line topology configuration should be found for several network sizes. This is achieved by the procedure listed in Table 1 assuming that  $\alpha=1$ .

Table 1: Calculation of Exact Hop-Count Distribution.

- ```

1) Begin
2)   input number of rings K
3)   h(1) = 4*K
4)   for i = 2 to 2*K
5)     h(i) = h(i-1) - 2
6)   end
7) End

```

At the end of this procedure, array  $\mathbf{h}$  contains the exact number of node pairs that are 1, 2, ...,  $2K$  hops apart. For example, when  $K=2$  then  $\mathbf{h}=[8 \ 6 \ 4 \ 2]$ . This means that

there are 8 pairs of nodes with hop-count 1, 6 pairs with hop-count 2, 4 pairs with hop-count 3, and 2 pairs with hop-count 4. When  $\mathbf{h}$  is found, then  $E[\mathbf{h}]$  can be easily determined. The above procedure is repeated for  $K=1$  ring to  $K=25$  rings, i.e.,  $N=3$  nodes to  $N=51$  nodes. For each value of  $N$ ,  $E[\mathbf{h}]$  is calculated and it is found to be a linear function of the node number  $N$  described in the following equation:

$$E[\mathbf{h}]_{\alpha=1} = \frac{N+1}{3} \quad (12)$$

When  $\alpha \neq 1$ , equation (12) computes the expected hop-count over relay nodes only. When a node that is not on a relay ring needs to transmit, it should first relay its traffic to a node on a relay ring. Therefore, if both source and destination are not on relay rings,  $E[\mathbf{h}]$  is 2 hops more than the expected hop-count over relay nodes.  $E[\mathbf{h}]$  is then:

$$E[\mathbf{h}] = \frac{N_r+1}{3} + 2\left(1 - \frac{N_r}{N}\right) \quad (13)$$

where  $N_r$  is number of relay nodes given in equation (4) and  $(1-N_r/N)$  is the probability that either the source or the destination node is not on a relay ring. Equation (13) is valid also when  $\alpha=1$  since  $N=N_r$  in this case.

## IV. CAPACITY CALCULATIONS

In general, the channel capacity  $C$  (in bits/s) between any two nodes in a network is governed by Shannon channel capacity formula [8] that can be expressed in the form:

$$C = W \cdot \log_2(1 + E[S/I]) \quad (14)$$

where  $W$  is the channel bandwidth and  $E[S/I]$  is the expected value of signal to interference ratio in the channel. However, the used transmission technique and medium access scheme impose some modifications to equation (14). A spread-spectrum system needs at least a bandwidth of  $W$  determined by the transmission bit rate  $r$ , but actually it uses a much larger bandwidth. Using much larger bandwidth will help in reducing the interference power by a factor called the *processing gain* [9, chapter 3] that we will refer to as  $g$ .

Medium access scheme will affect the channel capacity in two ways. Firstly, it will restrict the channel capacity by a *channel utilization factor* [4] denoted by  $u$ . Secondly, it will affect the calculations of interference in the network. In the following subsections we will find a closed-form formula for the channel capacity using equation (14) based on UWB and WLAN technologies.

#### A. UWB Ad Hoc Networks

When using TH-IR-UWB,  $u$  factor will be 1 since all nodes can use the medium at any time. In addition,  $g$  will reduce the interference power since spread-spectrum techniques are used in UWB technology.

### 1) Expected Interference Power

As seen in Fig. 1, the highest number of interfering nodes will be around the center node  $\mathbf{n}_0$ . Therefore, we will compute the total expected interference power  $E[I]$  experienced at  $\mathbf{n}_0$ . At node  $\mathbf{n}_0$  interference comes from all other nodes because we assume that all nodes in the network can transmit simultaneously. The  $j^{\text{th}}$  interfering ring contains 2 nodes at distance  $j \cdot \Delta$  from  $\mathbf{n}_0$ . Therefore, using equation (1), the accumulative expected power level of interference coming from all interfering nodes in the network reduced by the processing gain  $g$  is then:

$$\begin{aligned} E[I] &= \sum_{j=1}^K \frac{2p_{tr} \cdot c(j \cdot \Delta)^{-\beta}}{g} \\ &= \frac{2p_{tr} \cdot c \cdot \Delta^{-\beta}}{g} \sum_{j=1}^K j^{-\beta} \end{aligned} \quad (15)$$

where  $p_{tr}$  is the probability of packet transmission given by equation (8). When  $K \rightarrow \infty$ , equation (15) can be written as:

$$E[I] = \frac{2p_{tr} \cdot c \cdot \Delta^{-\beta}}{g} \zeta(\beta) \quad (16)$$

where  $\zeta(\beta) = \sum_{j=1}^{\infty} j^{-\beta}$  is the Riemann-Zeta function [10]. In wireless communications,  $\beta$  is always greater than 1. Hence,  $\zeta(\beta)$  is a convergence series and upper bounded by [11]:

$$\sum_{j=1}^{\infty} j^{-\beta} \leq \left( 1 + \int_1^{\infty} \frac{1}{x^{\beta}} dx \right) = \frac{\beta}{\beta-1} \quad (17)$$

Therefore,  $E[I]$  in TH-IR-UWB networks with line topology is upper bounded by:

$$E[I] \leq \frac{2p_{tr} \cdot c \cdot \Delta^{-\beta} \cdot \beta}{g(\beta-1)} \quad (18)$$

### 2) Expected Signal Power

The useful signal will come from one of the nodes that has a direct link with node  $\mathbf{n}_0$ , i.e., from a node inside the coverage area of  $\mathbf{n}_0$ . As seen in Fig. 1, there are  $2\alpha$  nodes within this area in addition to  $\mathbf{n}_0$ . For  $j \leq \alpha$ , the  $j^{\text{th}}$  ring contains 2 nodes at distance  $j \cdot \Delta$  from  $\mathbf{n}_0$ . The probability that the useful signal originated from the  $j^{\text{th}}$  ring is then  $2/2\alpha = 1/\alpha$ . Therefore, using equation (1), the expected power level of the useful signal taking into account all possible rings is given by:

$$\begin{aligned} E[S] &= \sum_{j=1}^{\alpha} \frac{c(j \cdot \Delta)^{-\beta}}{\alpha} \\ &= \frac{c \cdot \Delta^{-\beta}}{\alpha} \sum_{j=1}^{\alpha} j^{-\beta} \end{aligned} \quad (19)$$

### 3) Expected Channel Capacity

Using equations (15) and (19),  $E[S/I]$  is given by:

$$E[S/I] = \frac{g \sum_{j=1}^{\alpha} j^{-\beta}}{2\alpha \cdot p_{tr} \sum_{j=1}^K j^{-\beta}} \quad (20)$$

Substituting  $E[S/I]$  given by equation (20) in equation (14), the expected capacity of a link between two nodes inside the coverage area of each other is given by:

$$C = W \cdot \log_2 \left( 1 + \frac{g \sum_{j=1}^{\alpha} j^{-\beta}}{2\alpha \cdot p_{tr} \sum_{j=1}^K j^{-\beta}} \right) \quad (21)$$

where:

$$\begin{aligned} W &= r ; \\ p_{tr} &= 1 - \exp(-\lambda \cdot E[h]) ; \\ \lambda &= \frac{r_{in}}{r} ; \\ E[h] &= \frac{N_r + 1}{3} + 2 \left( 1 - \frac{N_r}{N} \right); \\ N_r &= 1 + 2 \left\lfloor \frac{K}{\alpha} \right\rfloor ; \\ K &= \frac{N-1}{2}; \quad N \text{ is always odd.} \end{aligned}$$

The capacity given by equation (21) represents  $r_{o,max}$  per node in UWB ad hoc networks with line topology configuration and TH-IR-UWB multiple access scheme. Hence, the maximum allowed input throughput per node  $r_{in,max}$  can be determined by equation (11).

We use equations (10) and (21) to plot the output throughput per node  $r_o$  showing the saturation points due to channel capacity  $C$  limit and transmission bit rate  $r$  limit. For example, 1Mb/s is a typical value of  $r$  as proposed by IEEE 802.15.4a group [12]. For indoor industrial application, we can choose  $\beta$  to be 2.15 for Non Line of Sight (NLOS) wireless communications. Let  $r_{in}$  be 50Kb/s. Using these values,  $r_o$  and  $C$  are plotted as functions of number of nodes  $N$  in the network. The plots are shown in Fig. 2 for different values of processing gain  $g$  and density of nodes represented by  $\alpha$ . Note that number of nodes considered in the figures is very common in a production line network scenario [1]. In this scenario, source-destination pairs are at most 5 hops apart and these pairs along the line interfere with each other. When  $\alpha=10$ , one should remember that number of relay nodes  $N_r$  is about 10 times less than number of nodes  $N$  in the network.

As shown in Fig. 2(a), the value of  $g$  affects significantly  $C$ . When  $g = 1$ , this denotes that there is no spreading of the signal power. Thus, there is no reduction of the interference level.

Consequently,  $C$  sinks to values lower than  $r$ . As a result,  $r_o$  is limited basically by channel capacity. However, when  $g = 100$ ,  $C$  becomes very large. In this case,  $r_o$  is limited by the transmission bit rate  $r$ . In UWB ad hoc networks  $g$  is very large and it could be around 5000. Thus, as expected, UWB ad hoc networks with line topology have very large channel capacity. As a result, the transmission bit rate is the main limit of output throughput per node  $r_o$  in such networks.

The density of nodes in the line topology can be increased by increasing the value of  $\alpha$ . If the nodes density increases, the interference level will increase as well. This will result in lower  $C$  as shown in Fig. 2(b). However, with the large value of  $g$ , UWB ad hoc networks with line topology still have very large channel capacity as indicated in Fig. 2(b), and the transmission bit rate is still the main limit of output throughput per node  $r_o$  in such networks.

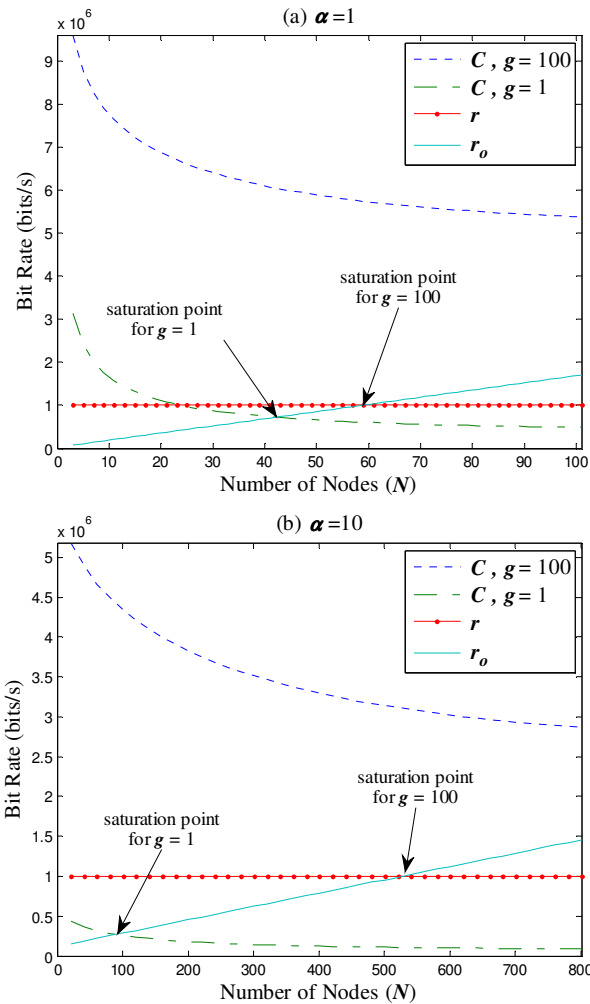


Fig. 2:  $r_o$  Limits in UWB Ad Hoc Networks.

### B. WLAN Ad Hoc Networks

If the basic form of CSMA/CA protocol is considered, the calculation of the channel capacity using equation (14) will be different. Assuming that transmission range equals to interference range, among  $(1+2\alpha)$  nodes inside the coverage

area of any node in the line topology, e.g.,  $\mathbf{n}_0$  in Fig. 1, only one node can transmit at a time. In this case,  $u$  factor equals to the reciprocal of  $(1+2\alpha)$ . Hence,  $C$  has to be divided by  $(1+2\alpha)$  to include  $u$  factor. The channel capacity is then:

$$C = \frac{W}{1+2\alpha} \log_2 (1 + E[S/I]) \quad (22)$$

The calculation of  $E[S]$  at  $\mathbf{n}_0$  is the same as in UWB ad hoc networks and it is given by equation (19). However, the calculation of  $E[I]$  is different. Let us calculate the total expected interference power  $E[I]$  experienced at  $\mathbf{n}_0$ . Since only one node is allowed to transmit inside the coverage area of  $\mathbf{n}_0$ , the first interfering ring is located just outside this coverage area, i.e., at distance  $(\alpha+1)\Delta$  from  $\mathbf{n}_0$ . The next interfering ring is located just outside the coverage area of the nodes on the previous interfering ring at distance  $(\alpha+1)\Delta$  from it. For  $j \leq \lfloor K/(\alpha+1) \rfloor$ , the  $j^{th}$  interfering ring contains 2 nodes at distance  $j(\alpha+1)\Delta$  from  $\mathbf{n}_0$ . Thus, using equation (1), the accumulative expected power level of interference coming from all interfering nodes in the network is given by:

$$\begin{aligned} E[I] &= \sum_{j=1}^{\lfloor K/(\alpha+1) \rfloor} \frac{2p_{tr} \cdot c (j(\alpha+1)\Delta)^{-\beta}}{g} \\ &= \frac{2p_{tr} \cdot c \cdot \Delta^{-\beta} (\alpha+1)^{-\beta}}{g} \sum_{j=1}^{\lfloor K/(\alpha+1) \rfloor} j^{-\beta} \end{aligned} \quad (23)$$

where  $p_{tr}$  is given by equation (8) and  $g$  is the processing gain since spread-spectrum techniques are also used in WLAN technology. When  $\lfloor K/(\alpha+1) \rfloor \rightarrow \infty$ ,  $E[I]$  for WLAN ad hoc networks with line topology is upper bounded by:

$$E[I] \leq \frac{2p_{tr} \cdot c \cdot \Delta^{-\beta} \cdot \beta (\alpha+1)^{-\beta}}{g(\beta-1)} \quad (24)$$

Using equations (19) and (23),  $E[S/I]$  is given by:

$$E[S/I] = \frac{g(\alpha+1)^\beta \sum_{j=1}^{\alpha} j^{-\beta}}{2\alpha \cdot p_{tr} \sum_{j=1}^{\lfloor K/(\alpha+1) \rfloor} j^{-\beta}} \quad (25)$$

Substituting  $E[S/I]$  given by (25) in (22), the expected capacity of a direct link between two nodes is given by:

$$C = \frac{W}{1+2\alpha} \cdot \log_2 \left( 1 + \frac{g(\alpha+1)^\beta \sum_{j=1}^{\alpha} j^{-\beta}}{2\alpha \cdot p_{tr} \sum_{j=1}^{\lfloor K/(\alpha+1) \rfloor} j^{-\beta}} \right) \quad (26)$$

The capacity given by equation (26) represents  $r_{o,max}$  per node in WLAN ad hoc networks with line topology configuration and CSMA/CA multiple access scheme. Hence,  $r_{in,max}$  can be determined by equation (11).

We use equations (10) and (26) to plot the output throughput per node  $r_o$  showing the saturation points due to channel capacity  $C$  limit and transmission bit rate  $r$  limit. For example, 1Mb/s is a typical value of  $r$  as proposed by IEEE 802.11 standard [7]. For indoor industrial application, we can choose  $\beta$  to be 2.15 for NLOS wireless communications. Let  $r_{in}$  be 50Kb/s. Using these values,  $r_o$  and  $C$  are plotted as functions of number of nodes  $N$  in the network. The plots are shown in Fig. 3 for different values of  $g$  and  $\alpha$ .

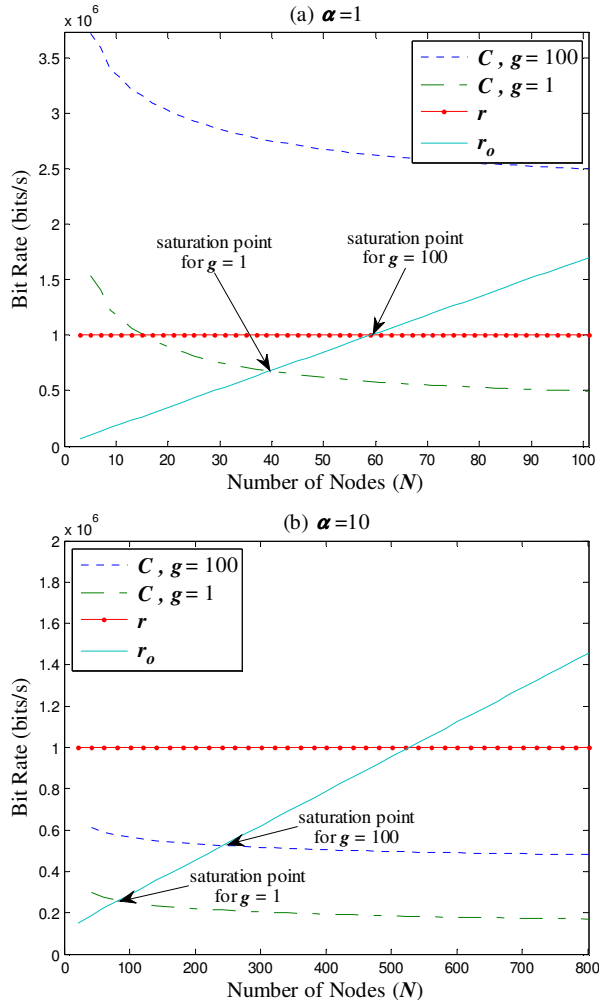


Fig. 3:  $r_o$  Limits in WLAN Ad Hoc Networks.

Comparing Fig. 3(a) with Fig. 2(a), we can see that at low density of nodes, the saturation points of  $r_o$  in WLAN ad hoc networks occur due to the same limits as in UWB ad hoc networks but at a different point for channel capacity limit with lower value. However, when the density of nodes increases,  $C$  decreases rapidly and becomes lower than the transmission bit rate  $r$  even for large values of  $g$ . In practice,  $g$  in WLAN is much lower than 100. A typical value of  $g$  is 11 as proposed by IEEE 802.11 standard [7]. Therefore, WLAN ad hoc networks

with line topology have very low channel capacity as indicated in Fig. 3(b) and channel capacity is the main limit of output throughput per node  $r_o$  in such networks. In other words, by comparing Fig. 2(b) with Fig. 3(b), we can see clearly that UWB technology outperforms WLAN technology in ad hoc networks with line topology.

## V. MODEL VERIFICATION

The line topology shown in Fig. 1 is simulated using ns-2 [13] version ns-allinone-2.29.3 running under SUSE Linux 10.1 operating system. WLAN technology operating with IEEE 802.11 standard [7] is implemented in the above ns-2 version. However, UWB technology is not implemented so far. Thus, the code version ns-2.29-uwb-0.10.0 is used [14] for UWB technology. The simulation time is 100s. Each simulation experiment is repeated 25 times and their average is used. The 99% confidence intervals for the simulation results are included in the plots. Our simulation codes and parameters default settings are freely available [15].

The line topology with 5 relay rings is simulated. Transmission range of all nodes  $R$  is fixed. Number of nodes in the topology depends on the value of  $\alpha$  and  $K$ . The value of  $\alpha$  is varied to take the values 1, 2 and 5; for  $K=5, 10$  and 25 respectively. Thus, the ratio  $K/\alpha$  is always 5, i.e., 5 relay rings. By increasing the value of  $\alpha$ , we increase node density in the network. For each of  $(\alpha, K)$  pair value, the input throughput per node  $r_{in}$  is varied to measure the saturation point of the simulated output throughput per node  $r_{o,sim}$ . The results are shown in Fig. 4 and Fig. 5 for WLAN and UWB technologies respectively. In these figures, the channel capacity  $C$  and the transmission bit rate  $r$  are also plotted.

In Fig. 4, the theoretical and simulated  $r_o$  is plotted versus  $r_{in}$  using WLAN technology.  $r_{o,thr}$  is plotted using equation (10). Also,  $C$  is plotted using equation (26). In these plots,  $r$  is 1Mb/s and  $\beta$  is 2. With these settings,  $r_{o,thr}$  and  $r_{o,sim}$  are plotted for  $\alpha=1, 2$  and 5; while  $K=5, 10$  and 25 respectively. As shown in Fig. 4,  $r_{o,sim}$  increases along with  $r_{o,thr}$  as  $r_{in}$  increases until the saturation point of channel capacity is reached. After this saturation point,  $r_{o,sim}$  starts to sink and it is then limited by channel capacity. This is true for the three cases, i.e., for  $\alpha=1, 2$  and 5. It is noticed that the simulated saturation point is a little bit higher than the theoretical value. This is because re-transmissions due to packet loss and collisions are not included in the mathematical model, but it is included in the simulation and this is a source of error. However, this will mainly affect packet transmission probability  $p_{tr}$  at low  $r_{in}$ . Including re-transmissions will increase traffic in the network, and hence,  $p_{tr}$  will increase. But as  $r_{in}$  becomes large,  $p_{tr}$  reaches its upper bound value which is 1 and re-transmissions will not affect our model anymore. Therefore, for large  $r_{in}$ , we expect that  $r_{o,sim}$  will converge to the same value as  $C$  especially for large values of  $\alpha$ . This behavior is noticed in  $r_{o,sim}$  as shown in Fig. 4.

In Fig. 5, the theoretical and simulated  $r_o$  is plotted versus  $r_{in}$  using UWB technology.  $r_{o,thr}$  is plotted using equation (10).  $C$  is not shown since it is much larger than  $r$ . In these plots,  $r$  is 1Mb/s and  $\beta$  is 2. With these settings,  $r_{o,thr}$  and  $r_{o,sim}$  are plotted for  $\alpha=1$ ; while  $K=5$ . As shown in Fig. 5,  $r_{o,sim}$  increases along

with  $r_{o,thr}$  as  $r_{in}$  increases until the saturation point of transmission bit rate  $r$  is reached. After this saturation point,  $r_{o,sim}$  starts to sink and it is then limited by the transmission bit rate  $r$ . The saturation point due to channel capacity is not shown in the plot since it is much larger than the transmission bit rate  $r$ .

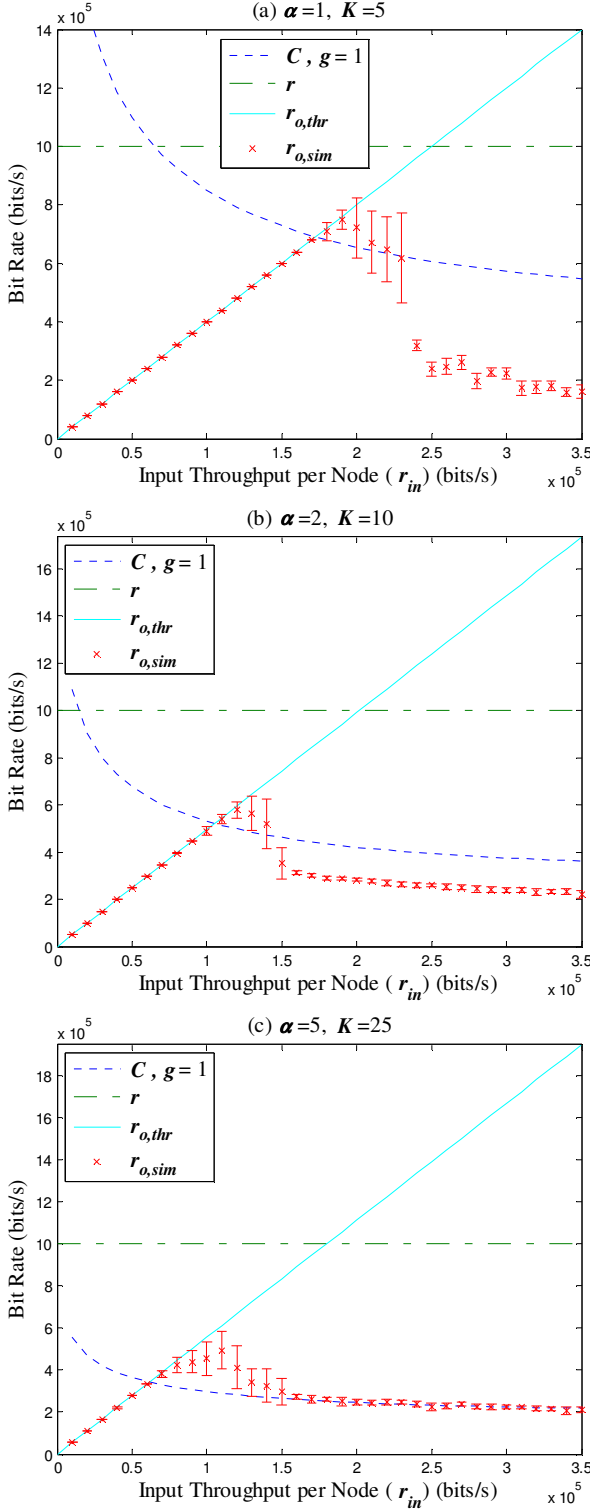


Fig. 4: Simulated  $r_o$  using WLAN Technology.

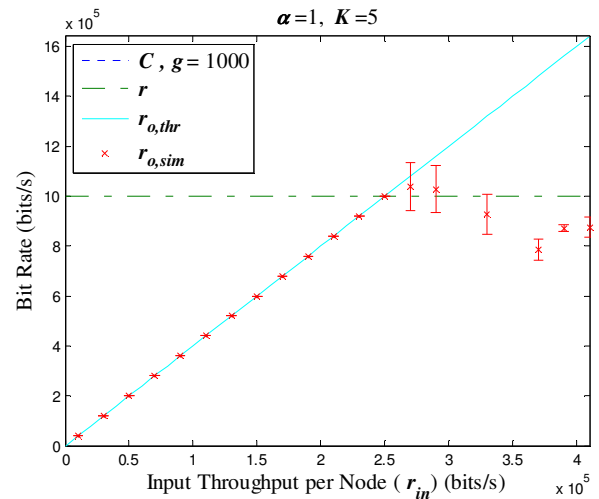


Fig. 5: Simulated  $r_o$  using UWB Technology.

The simulation results shown in Fig. 4 and Fig. 5 verify our mathematical model. Also, it is worth noting that our finding regarding the maximum input throughput per node  $r_{in,max}$  given in equation (11) agrees with results found in literature. For example, in [2],  $r_{in,max}$  (or the throughput capacity per node as called by the authors) is found to be in the form  $O(1/\sqrt{N})$ . In [16], the author shows that  $E[\mathbf{h}]$  of the network topology used in [2] is  $O(\sqrt{N})$ . Therefore,  $r_{in,max}$  for wireless networks with topology used in [2] according to (11) is  $O(1/\sqrt{N})$ . Furthermore, our analytical calculations regarding  $r_o$  comply with the simulation results found in studies that used the line topology. For example, it is found in [1] that if UWB technology is used instead of WLAN technology, the network throughput of the line topology will be much larger. Also, our analytical calculations regarding  $r_o$  comply with (or can explain) the simulation results obtained in [17] which uses also the line topology.

## VI. MODEL RESTRICTIONS

In our model, the channel capacity is calculated for the networks with line topology in which the nodes are distributed uniformly. Hence, this calculation will not be valid if the uniform distribution is disrupted. Also, our model assumes that the nodes are fixed in their locations. However, the calculation of the channel capacity remains valid as long as uniform distribution of nodes is not affected by moving nodes. In spite of this restriction, our model is applicable and can be used in the production line application described in [1], in which the network consists of moving nodes that are uniformly distributed along a line topology.

In addition, re-transmissions due to packet loss and collisions are not included in traffic. This will mainly affect packet transmission probability  $p_{tr}$ . However, regardless the exact expression of  $p_{tr}$ , we can explain the effect of it on channel capacity computation. Including re-transmissions will increase traffic in the network, and hence,  $p_{tr}$  will increase. With higher  $p_{tr}$ , the channel capacity will decay more rapidly.

but it will always converge to the same value since  $p_{tr} \leq 1$ . This behavior is verified using equations (21) and (26). In this context, our model still gives a lower bound for channel capacity when  $p_{tr}=1$  in case of full network load or excessive data traffic.

Finally, we assume that the pathloss power law model for radio propagation is used. This assumption is not practical under fading conditions and a more realistic pathloss model should be considered, e.g., a pathloss shadowing model. This is the main limitation of our model based on results obtained in [1].

## VII. SUMMARY AND CONCLUSIONS

In this paper closed-form formulas are found for the channel capacity of ad hoc networks with line topology based on UWB and WLAN technologies. The starting point for the computation is the Shannon channel capacity equation. However, an additional restriction on channel capacity is imposed by the multiple access scheme used in the network. Furthermore, the used multiple access scheme and spread-spectrum technique affect the calculation of interference level.

It is found that the capacity of ad hoc network with line topology depends on number of nodes, density of nodes, processing gain, hop-count distribution, and data traffic. It is also found that interference level is upper bounded for large network size. Therefore, the capacity is lower bounded. In case of ad hoc networks with line topology based on UWB technology, the upper bound of interference depends on probability of packet transmission, average power of transmission, distance between nodes, pathloss exponent, and processing gain as it can be seen from equation (18). Thus, even for excessive data traffic, the interference will be still upper bounded since the probability of packet transmission will not exceed 1. In case of WLAN technology, and assuming the same data traffic, power transmission, distance between nodes, and processing gain as in UWB technology, the interference upper bound expressed in equation (24) is reduced by a factor of  $(\alpha+1)^{-\beta}$  which is always less than 1 since  $\alpha$  and  $\beta$  are always greater than or equal to 1.

However, the channel capacity of ad hoc networks with line topology based on WLAN technology is much lower than that based on UWB technology for the same scenario especially for a high density of nodes. This is due to the fact that the channel inside a certain coverage area in WLAN is shared by many nodes and only one node among them can access the channel at a time. In contrast, with UWB technology the channel can be accessed by all nodes simultaneously. In addition, UWB technology has a much larger processing gain. As a result, the output throughput per node  $r_o$  is limited mainly by the transmission bit rate  $r$  in case of UWB technology. On the other hand,  $r_o$  is limited mainly by channel capacity in case of WLAN technology.

Our model is derived for the line topology configuration which can be used in a vital industrial indoor application, e.g., a production line in a factory. Following a similar systematic

model, the channel capacity can be found for other topology configurations as well.

One more conclusion is that the channel capacity is maximized when routing is done using the energy conservation method, i.e., when  $\alpha=1$ . This method will ensure that the minimum number of nodes inside the coverage area of a node is used. Therefore, the interference level will be minimized.

Finally, this work presents a simple systematic model by which the factors affecting channel capacity can be easily controlled to understand their role in channel capacity computations. The main restriction of this model is the pathloss power law model used for radio propagation. This pathloss model is not practical for industrial indoor applications. Therefore, as a future work, it is intended to consider a more realistic pathloss model such as shadowing (or fading) model.

## REFERENCES

- [1] S. Bali, J. Steuer and K. Jobmann, "Performance of Three Routing Protocols in UWB Ad Hoc Network Deployed in an Industrial Application," *GLOBECOM'07: IEEE Workshop on Wireless Mesh and Sensor Networks*, 30 Nov, 2007.
- [2] P. Gupta and P. R. Kumar, "The Capacity of Wireless Networks," *IEEE Transactions on Information Theory*, vol. 46, no. 2, pp. 388-404, 2000.
- [3] R. Negi and A. Rajeswaran, "Capacity of Power Constrained Ad-hoc Networks," in *Proceedings of IEEE INFOCOM'04*, pp. 443-453, 2004.
- [4] R. Hekmat and P. V. Mieghem, "Interference in Wireless Multi-hop Ad-hoc Networks and its Effect on Network Capacity," *Wireless Networks Journal*, vol. 10, No. 4, pp. 389-399, 2004.
- [5] R. Prasad, *Universal Wireless Personal Communications*, Artech House Publishers, 1998.
- [6] M. Z. Win and R. A. Scholtz, "Ultra-Wide Bandwidth Time-Hopping Spread-Spectrum Impulse Radio for Wireless Multiple-Access Communication," *IEEE Trans. On Comm.*, vol. 48, pp. 679-690, 2000.
- [7] Supplement to IEEE Standard 802.11-1999, "Part-11: Wireless LAN Medium Access Control (MAC) and Physical Layer (PHY) Specification: High-speed Physical Layer in 5 GHz Band," IEEE standard 802.11a-1999.
- [8] C. E. Shannon, "A Mathematical Theory of Communications," *Bell System Technical Journal*, vol. 27, pp. 379-423 and 623-656, July and October, 1948.
- [9] I. Oppermann, M. Haemaelaeinen and J. Iinatti, *UWB Theory and Applications*, John Wiley and Sons, 2004.
- [10] M. Abramowitz; I. R. Stegun, *Handbook of Mathematical Functions*, Dover Publications, 1970.
- [11] C.H. Edwards and D. E. Penney, *Calculus with Analytic Geometry*, Prentice-Hall, 1994.
- [12] <http://www.ieee802.org/15/pub/TG4a.html>
- [13] <http://www.isi.edu/nsnam/ns>
- [14] <http://icawww1.epfl.ch/uwb>
- [15] <http://www.ikt.uni-hannover.de/index.php?id=publikationen0>
- [16] R. Hekmat, *Ad-hoc Networks: Fundamental Properties and Network Topologies*, Springer, 2006.
- [17] J. Li, C. Blake, D. De Couto, H. Lee and R. Morris, "Capacity of Ad Hoc Wireless Networks," in *Proceedings of the 7th ACM International Conference MobiCom '01*, pp. 61-69, July 2001.